Surface convergence zones due to Lagrangian residual flow in tidally driven estuaries

Tobias Kukulka[a] and Robert J. Chant[b]

[a] *University of Delaware, Newark, Delaware, USA*

[b] *Rutgers University, New Brunswick, New Jersey, USA*

Corresponding author: Tobias Kukulka, kukulka@udel.edu

ABSTRACT: Buoyant material, such as floating debris, marine organisms, and spilled oil, is aggregated and trapped within estuaries. Traditionally, the aggregation of buoyant material is assumed to be a consequence of converging Eulerian surface currents, often associated with lateral (cross-estuary) density gradients that drive baroclinic lateral circulations. This study explores an alternative aggregation mechanism due to tidally driven Lagrangian residual circulations without Eulerian convergence zones and without lateral density variation. In a tidally driven estuary, the depth-dependent tidal phase of the lateral velocity varies across the estuary. This study demonstrates that the lateral movement of surface trapped material follows the tidal phase, resulting in a lateral Lagrangian residual circulation known as Stokes drift for small amplitude motions. For steeper bathymetry, the lateral change in tidal phase is greater and the corresponding lateral Lagrangian residual flow faster. At local depth extrema, e.g. in the thalweg, depth does not vary laterally, so that the associated tidal phase is laterally constant. Therefore, the Stokes drift is weak near depth extrema resulting in Lagrangian convergence zones where buoyant material concentrates. These ideas are evaluated employing an idealized analytic model in which the along-estuary tidal flow is driven by an imposed barotropic pressure gradient, whereas cross-estuary flow is induced by the Coriolis force. Model results highlight that convergence zones due to Lagrangian residual velocities are efficient in forming persistent aggregation regions of buoyant material along the estuary.

SIGNIFICANCE STATEMENT: Our study focuses on the aggregation of buoyant material (e.g., debris, oil, organisms) in estuaries. Traditionally, the aggregation of buoyant material is assumed to be a consequence of converging Eulerian surface currents, often associated with lateral (cross-estuary) density gradients that drive baroclinic lateral circulations. Our study explores an alternative aggregation mechanism due to tidally driven Lagrangian residual circulations without Eulerian convergence zones and without lateral density variation. Our results highlight that convergence zones due to Lagrangian residual velocities are efficient in forming persistent aggregation regions of buoyant material along the estuary.

1. Introduction

The estuarine circulation transports buoyant material such as floating debris, marine organisms, surface foam, air bubbles, and pollutants, e.g., oil and microplastics (Kennish 2002). Previous observations and hydrodynamic simulations indicate that buoyant material concentrates in laterally narrow near-surface patches that may extend from several 100 meters to a few kilometers along the estuary (e.g., Nunes and Simpson 1985; Cohen et al. 2019). These material patches greatly facilitate interactions between particles related to mating behavior, predator-prey dynamics, access to nutrients, and the exposure to pollutants. A common mechanism for patch formation is attributed to converging near-surface currents as part of the Eulerian estuarine circulation (e.g., Nunes and Simpson 1985; MacCready and Geyer 2010). This study explores an alternative aggregation mechanism due to tidally averaged Lagrangian residual flow (Zimmerman 1979).

Eulerian surface convergence flows can be induced by lateral density variability, for example, resulting from differential advection during a tidal cycle (Nunes and Simpson 1985; MacCready and Geyer 2010). During flood, density in the thalweg becomes elevated relative to the flanks and the resulting baroclinic torques drive a two-cell flow structure with lateral surface currents towards the channel center (Lerczak and Geyer 2004; Burchard et al. 2011; Li et al. 2014). This mechanism suggests that along-estuary surface aggregation zones are tightly linked to lateral density variability. Here, we demonstrate that aggregation zones can form independently of the lateral density distribution.

The Coriolis force presents another critical ingredient in driving flows across the estuary (Lerczak and Geyer 2004; Valle-Levinson 2008; Li et al. 2014). The cell structure of this lateral circulation

can be complex and generally depends on the estuary geometry, turbulent mixing, and density variations. For example, Lerczak and Geyer (2004) explore a single lateral circulation cell due to tidally varying Ekman dynamics. Such circulations are associated with vanishing tidally averaged Eulerian velocities. However, this study finds that in a Lagrangian framework, Eulerian currents with zero tidal average nevertheless contribute to particle transport due the lateral Lagrangian residual velocities. The Lagrangian residual velocity is defined as the velocity of a marked fluid parcel averaged over one tidal cycle (Longuet-Higgins 1969; Zimmerman 1979).

The importance of the Lagrangian framework to understand mass transport by time-varying ocean currents has long been recognized (Longuet-Higgins 1969; Zimmerman 1979); yet, except for a handful of exceptions (e.g., Feng et al. 1986; Jay 1991; Ridderinkhof and Zimmerman 1992; Lemagie and Lerczak 2015), few studies previously explored a Lagrangian approach to estuarine transport. A tidally averaged Lagrangian residual velocity (Stokes drift velocity for small amplitude motions) in the direction of phase progression of the oscillatory currents is well known to occur for surface waves including tides (Longuet-Higgins 1969; Li and O'Donnell 1997; LeBlond 1978). This study shows that time-dependent secondary flows in estuaries result in Lagrangian residual flows that laterally organizes buoyant material and controls material transport, playing an important role in estuarine transport processes.

To understand the Stokes drift intuitively it is insightful to cite Chris Garrett (2004): "The Stokes drift is like surfing. The more you stay with a wave, the more you drift forward; that is, you stay longer with the forward flow than if were standing still (Eulerian) in which case you would see the forward and backward flow for exactly the same amount of time." A time-series of surface cross-channel velocities v_0 further illustrates this concept (Figure 1). Because the phase of v_0 depends on cross-estuary location y, the particle of the shown path (black line) spends more time in positive v_0 than in negative v_0, so that the particle moves forward over a tidal cycle by "surfing" positive v_0.

Laterally varying surface currents organize buoyant material and thus play an important role in estuarine transport processes. For example, Burchard et al. (2011) provide examples where the Eulerian mean flows at the surface in the channel center can either be (a) landward or (b) seaward depending on the details of the controlling dynamics. As such, a steady convergence of surface

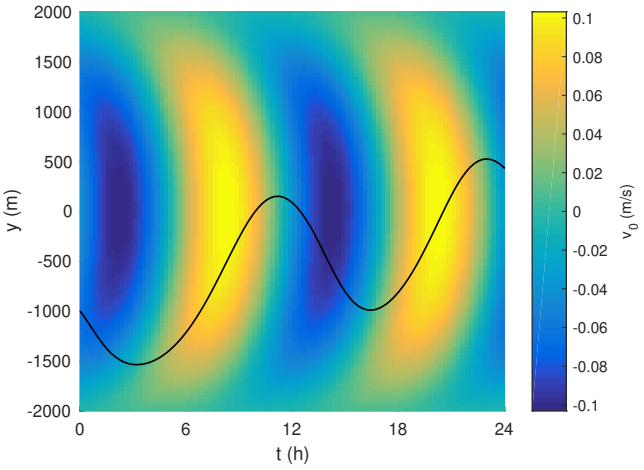

FIG. 1. Modeled cross-estuary surface velocity $v_0(t, y)$ as function of time t and cross-estuary location y with associated particle trajectory (black line). This trajectory shows how the particle released at $y = -1000$ m follows the phase to converge in an oscillating tidal motion over the channel center. The model is discussed in detail in section 3 and is based on solution (9) with parabolic bathymetry (Figure 2) with $h_{\max} = 15$ m and $h_{\min} = 5$ m and half width $B = 2$ km. Other model parameters are $A = 0.0022\text{m}^2\text{s}^{-1}$, U_0=0.75ms^{-1}, $f = 10^{-4}\text{s}^{-1}$.

material to the thalweg via lateral Stokes drift would result in the (a) retention or (b) export of material.

The goal of this paper is to provide a proof-of-concept demonstrating the importance of Lagrangian residual flows in tidally driven estuaries for aggregating buoyant material in laterally narrow zones along the estuary. The following section introduces basic theoretical concepts and discusses favorable conditions for converging Lagrangian flows in estuaries. Section 3 reviews an idealized analytic model for the tidally driven estuarine circulation following Lerczak and Geyer (2004), which is applied in section 4. We conclude in section 5 that Lagrangian convergence zones are efficient in forming persistent aggregation regions of buoyant material in estuaries.

2. Theory

a. Lagrangian residual velocity

We explore the horizontal Lagrangian residual velocity of an oscillating tidal flow with along-estuary velocity $u(t, y, z)$ and cross-estuary velocity $v(t, y, z)$. The velocity shall only depend on vertical coordinate (increasing upward with $z = 0$ at that air-sea interface) and on cross-estuary

(lateral) coordinate y (with $y = 0$ at the channel center), see definition sketch in Figure 2. The velocity (u, v) is assumed to be independent of the along-channel location x. The dependence of u and v on time t shall be prescribed by a sinusoidal oscillation, so that the Eulerian average $\bar{u}$ and $\bar{v}$ over one tidal cycle is zero that is $\bar{u} = \bar{v} = 0$. Here, the overbar denotes the temporal average over one tidal period T from $t - T/2$ to $t + T/2$.

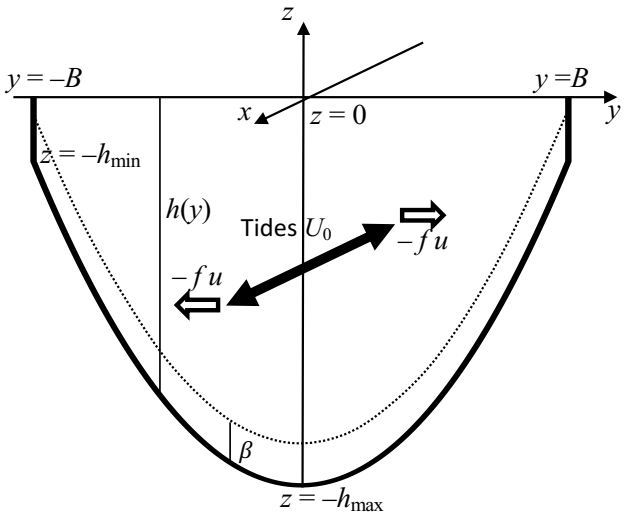

FIG. 2. Definition sketch of idealized estuary with parabolic cross-estuary bathymetry. Along-channel tidal currents are characterized by velocity scale U_0, the Coriolis force $-fu$ drives a cross-channel flow, while turbulent mixing induce a bottom boundary layer whose height scales as β. These processes result in a tidal cross-channel velocity whose phase depends on depth h.

The Lagrangian velocity is often decomposed in Eulerian and Stokes drift velocities (e.g., Buhler 2009). This decomposition is particularly meaningful for small amplitude motions in which the Stokes drift is the first order approximation of the difference between Lagrangian and Eulerian velocity. Following Longuet-Higgins (1969) and Zimmerman (1979), we distinguish in this study between Stokes drift for small amplitude motions and a more general residual circulation, which is the Lagrangian velocity with zero Eulerian mean motion.

To define the Lagrangian residual velocity, we first consider the time-dependent horizontal trajectory $(X(t), Y(t))$ of a particle marked at time t_0 and horizontal position (X_0, Y_0). For this

proof-of-concept study, we examine only Lagrangian surface motion with $z = 0$. The corresponding Lagrangian particle velocity is then obtained from the Eulerian velocity fields through the relation $(U,V) = (u(t,Y,0), v(t,Y,0))$. Finally, the Lagrangian residual velocity is defined by the tidal average of the Lagrangian velocity, $(\bar{U},\bar{V})$, where the overbar indicates the tidal average (Zimmerman 1979). In this study, we focus on convergence regions of $\bar{V}$; the explicit expression for $\bar{V}$ is

$$\bar{V}(t,t_0,Y_0) = \frac{1}{T}\int_{t-T/2}^{t+T/2} V(t',t_0,Y_0)dt' = \frac{1}{T}\int_{t-T/2}^{t+T/2} v(t',Y(t',t_0,Y_0),0)dt'. \tag{1}$$

b. Lagrangian convergence regions

To understand surface aggregation of buoyant particles due to Lagrangian convergence regions, we first approximate (1). For sufficiently small $|Y - Y_0|$, so that $|\sigma^{-1}\partial v/\partial y| \ll 1$, where $\sigma = 2\pi/T$ is the angular tidal frequency, the first order Taylor expansion in $(Y - Y_0)$ accurately approximates $\bar{V}$, which is referred to as Stokes drift v_s (Longuet-Higgins 1969)

$$\bar{V}(y) \approx v_s(y) = \overline{\frac{\partial v}{\partial y}(t',y)\int_{t-T/2}^{t'} v(t'',y)dt''}. \tag{2}$$

The condition $|\sigma^{-1}\partial v/\partial y| \ll 1$ ensures that lateral changes of v are relatively small over a tidal excursion. Generally v_s depends on estuary depth. Note that the Stokes drift does not depend on t because v is periodic over T and the range of motion is assumed to be sufficiently small in (2). For a sinusoidally varying tidal flow, the Eulerian cross-estuary velocity can be expressed as

$$v = |v|\Re\{\exp[i(\varphi - \sigma t)]\}, \tag{3}$$

where $|v|$ represent the cross-estuary velocity magnitude and φ denotes the cross-estuary velocity phase, $\Re$ symbolizes the real part of the argument. Substitution of this velocity expression into (2) yields

$$v_s = \frac{1}{2}\frac{|v|^2}{\sigma}\frac{\partial\varphi}{\partial y}, \tag{4}$$

which demonstrates that the lateral Stokes drift critically depends on the cross-estuary phase change $\partial\varphi/\partial y$. Generally, v depends on estuary depth h while $h(y)$ changes across the estuary (Figure 2),

so that the phase change becomes

$$\frac{\partial \varphi}{\partial y} = \frac{\partial \varphi}{\partial h}\frac{\partial h}{\partial y}. \tag{5}$$

The last equation suggests that the Stokes drift (4) is proportional to the channel slope $h_y = \partial h/\partial y$ so that the Lagrangian residual transport is greater for steeper bathymetry. Furthermore, wherever h has a local maximum, e.g. in the channel center (Figure 2), h_y changes its sign across that local maximum. Consequently, the Stokes drift flips sign as well, providing a mechanism for Lagrangian convergence zones over bathymetry extrema. Note that this result is valid for arbitrary cross-estuary depth profile $h(y)$ with a local maximum and does not dependent on any idealized parabolic channel geometry. Below we show that this mechanism is likely to occur in wide range of tidally driven estuaries that are wide enough for the Coriolis force to be important with sufficiently steep topography. In addition, $\varphi(h)$ may have a local extreme point along varying depth such that $\partial\varphi/\partial h = 0$, providing another possibility for Stokes drift convergence across the channel that is not related to bathymetry extrema but may occur away from the channel center in Figure 2. These possibilities for Lagrangian convergence will next be explored through an idealized model for Ekman-forced lateral flows.

3. Idealized model for Ekman-forced lateral flow

To design a straight-forward concept model with $\varphi(h)$ and $\bar{v} = 0$, we employ the idealized model for tidally driven Ekman-forced flow from Lerczak and Geyer (2004, see appendix therein), which is reviewed here for convenience. The governing linear equations for the tidally varying along- and cross-estuary velocities, u and v, respectively, are

$$\frac{\partial u}{\partial t} = -g\frac{\partial \eta}{\partial x} + A\frac{\partial^2 u}{\partial z^2}, \tag{6}$$

$$\frac{\partial v}{\partial t} = -f\left(u - \frac{1}{h}\int_{-h}^{0} u dz\right) + A\frac{\partial^2 v}{\partial z^2} + \frac{\tau_b}{h\rho}. \tag{7}$$

Here, the density ρ is assumed to be constant, f is the Coriolis parameter, A is a constant vertical eddy viscosity, g is the acceleration due to gravity, η is the sea-surface height, $\tau_b = \rho A(\partial v/\partial z)|_{z=-h}$ is the bottom stress, x is the along-estuary coordinate such that $x = 0$ at the estuary mouth and $x < 0$ up-estuary (Figure 2). The along-channel flow is driven by a prescribed tidally-varying hydrostatic

pressure gradient due to the sloping air-sea interface such that

$$\frac{\partial \eta}{\partial x} = \Re[iU_0 \sigma g^{-1} \exp(-i\sigma t)],$$

where U_0 is a constant scale for the tidal velocity amplitude and σ denotes the angular tidal frequency. The cross-channel flow is forced through the Coriolis term $-fu$ in (7). Note that (7) describes the dynamics of lateral flows by subtracting the depth average of the v equation assuming a negligible depth-average v.

The balance (7) highlights that the phase of v critically depends on depth h, which is directly seen by scaling the acceleration term (first left-hand side term) relative to the stress terms (two last right-hand side terms) whose ratio scales as h/β, where β is the boundary layer thickness $\beta = \sqrt{2A/\sigma}$ For relatively small h, $h/\beta \ll 1$, the acceleration term is relatively small, and v is expected to be in phase with the Coriolis term. On the other hand, for relatively large h, $h/\beta \gg 1$, acceleration is expected to be dominant so that v is 90° out of phase with the Coriolis term. Therefore, φ depends on h which results in a lateral Stokes drift if h varies across the estuary, as discussed above.

Solutions to (6) and (7) are derived by imposing the boundary conditions $u = v = 0$ at $z = -h$ and a zero surface stress condition $\partial u/\partial z = \partial v/\partial z = 0$ at $z = 0$ (see details in Lerczak and Geyer 2004). Furthermore, solutions are determined so that the depth-integrated cross-channel transport is zero for all t. Analytic solutions are obtained by imposing a time dependence $\exp(-i\sigma t)$ for u and v resulting with (6) and (7) in the complex cross-channel flow structure functions for v in (3)

$$|v|\exp(i\varphi) = \frac{i}{2} U_0 \frac{f}{\sigma}\left[\alpha \frac{\cosh(\kappa z)}{\cosh(\kappa h)} - \alpha \frac{\tanh(\kappa h)}{\kappa h} - \kappa z \frac{\sinh(\kappa z)}{\cosh(\kappa h)} - \frac{\tanh(\kappa h)}{\kappa h} + 1\right] \quad (8)$$

with $\kappa^2 = -2i\beta^{-2}$ and $\alpha = [(\kappa h)^2 \tanh(\kappa h)]/[\kappa h - \tanh(\kappa h)] - 1$. The lateral velocity depends on the non-dimensional boundary layer thickness β/h (Figure 3). If β is comparable to h, the lateral velocity is characterized by a single lateral cell structure, whereas for small β and greater h/β, the boundary layer is shallower and cross-currents intensify closer to the bottom (Lerczak and Geyer 2004).

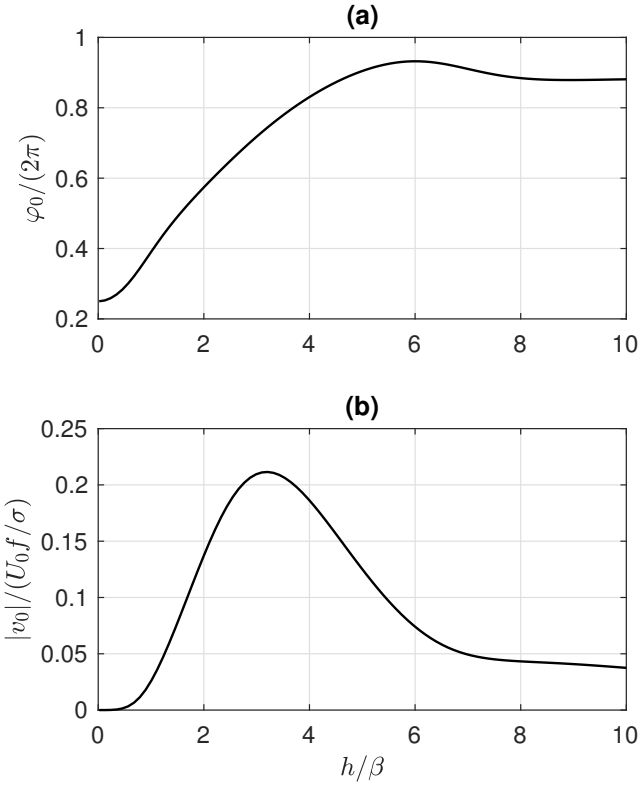

FIG. 3. Non-dimensional lateral surface (a) phase φ_0 and (b) velocity magnitude $|v_0|$ from (9) as a function of non-dimensional depth h/β. For constant β, the phase φ_0 changes as the particle moves accross the estuary resulting in a Stokes drift according to (4).

In this study, we are interested in the lateral surface velocity $v_0 = v(z=0)$ with phase $\varphi_0 = \varphi(z=0)$ which are normalized as

$$\frac{\sigma}{f}\frac{|v_0|}{U_0}\exp(i\varphi_0) = \frac{i}{2}\left[\frac{\alpha}{\cosh(\kappa h)} - \alpha\frac{\tanh(\kappa h)}{\kappa h} - \frac{\tanh(\kappa h)}{\kappa h} + 1\right]. \tag{9}$$

Thus, the normalized surface velocity magnitudes and phases only depend on h/β because $\kappa \propto \beta^{-1}$ (Figure 3). Lerczak and Geyer (2004) considered the range of $0.1 < \beta/h < 0.4$ or $2.5 < h/\beta < 10$, which is typical range found in estuarine systems. For this parameter range, Figure 3 suggests a significant $|v|$ and a substantial dependence of φ on h for $h/\beta > 8$, indicating non-zero Stokes drift according to (4) and a significant Lagrangian residual circulation. Figure 1 illustrates how the lateral surface velocity v_0 changes over a tidal cycle across the estuary enabling surface trapped particles to move with the phase.

4. Convergence zones due to the Lagrangian residual circulation

Applying the idealized model, we will first contrast differences between the Stokes drift and the full Lagrangian residual velocity, before considering illustrative example solutions for a parabolic cross-estuary bathymetry (Figure 2).

a. Stokes drift

Substitution of (8) into (4) results in the non-dimensioan lateral Stokes drift

$$v_s \frac{\beta\sigma}{(U_0 f/\sigma)^2}\frac{1}{h_y} = \frac{1}{2}\frac{|v|^2}{(U_0 f/\sigma)^2}\frac{\partial\varphi}{\partial(h/\beta)}, \tag{10}$$

which only depends on the single non-dimensional parameter (h/β) (Figure 4). The normalized Stokes drift peaks near where $|v|$ and $\partial\varphi/\partial(h/\beta)$ peak, compare with Figure 3. Note that the Stokes drift changes sign near $h/\beta = 6$, which is associated with a Lagrangian convergence zone as discussed above. Equation (10) highlights that the Stokes drift is proportional to h_y. Recall that h_y must not be too large for an accurate Stokes drift estimate because the small amplitude motion requires that v does only change approximately linearly along the particle $Y - Y_0$. This requires that $|\sigma^{-1}\partial v/\partial y| \ll 1$ or $h_y(\beta\sigma)^{-1}|\partial v/\partial(y/\beta)| \ll 1$, so that h_y also critically controls higher order contributions to the Lagrangian residual velocity (1).

b. Dependence of $\bar{V}$ on h_y and h/β

Next we release and track particles for the flow field (9) to determine the Lagrangian residual circulation numerically based on (1) (Figure 4). Particle paths are computed using standard numerical ordinary differential equation solvers (4th order Runge-Kutta method). Solutions are obtained over a range of the two independent parameters h/β and h_y, where h_y is set constant for each run. The Lagrangian residual velocity still peaks close to where $|v|$ and $\partial\varphi/\partial y$ peak, compare with Figure 3, but clearly also depends on slope h_y (Figure 4). As expected, the Stokes drift (10) accurately approximates $\bar{V}$ for smaller slopes. These numeric solutions provide an expectation for $\bar{V}$ and Lagrangian convergence zones $\partial\bar{V}/\partial y < 0$ across the channel for given β and $h(y)$.

For realistic parameters (for example, Figure 4a with h_y=0.01, $A = 0.0022\mathrm{m}^2\mathrm{s}^{-1}$, U_0=0.75ms^{-1}, $f = 10^{-4}\mathrm{s}^{-1}$) we find $\bar{V}$ in the order of several cm/s, which comparable to tidally averaged Eulerian

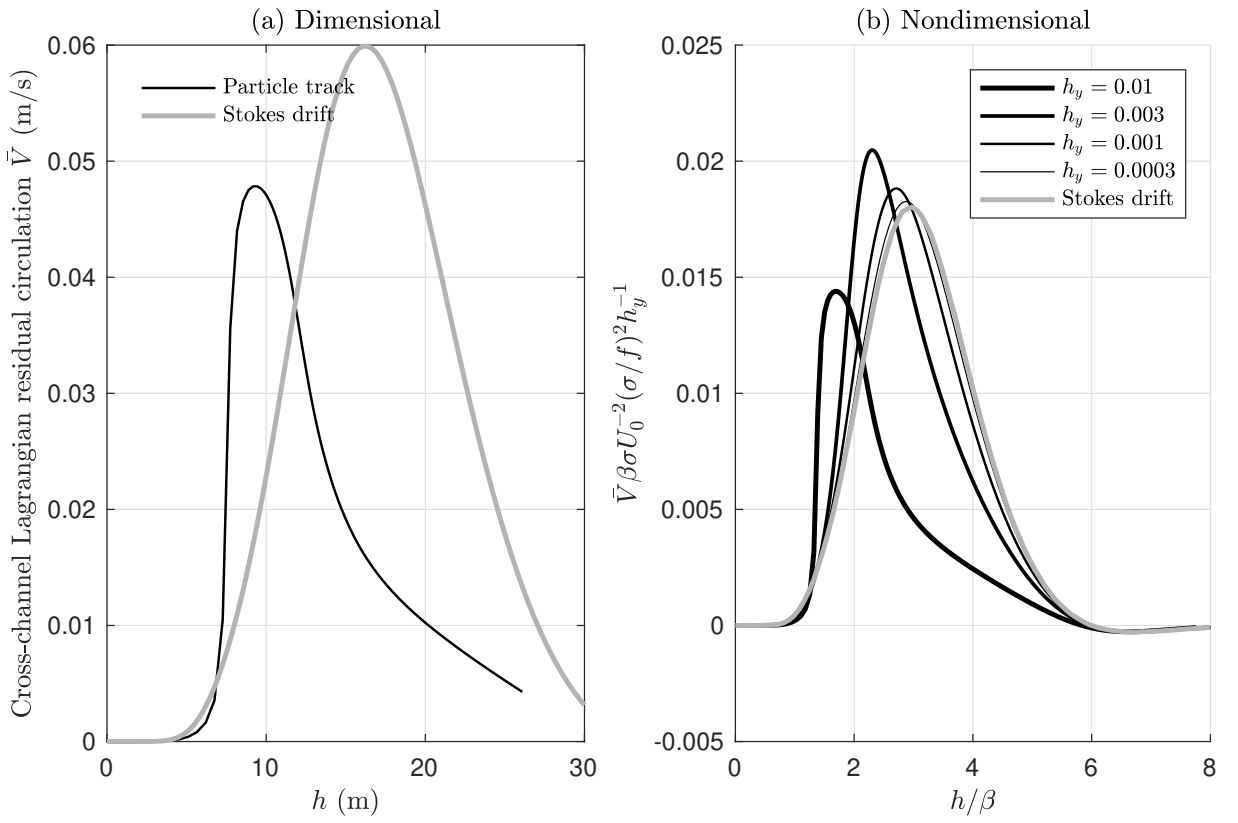

FIG. 4. Cross-channel Lagrangian residual velocity $\bar{V}$ from (1) for (a) a dimensional example and (b) non-dimensional $\bar{V}\beta\sigma/(U_0 f/\sigma)^2/h_y$ which depends only on h/β and h_y. Gray line shows the Stokes drift estimate (10). The dimensional case uses parameters h_y=0.01, $A = 0.0022\text{m}^2\text{s}^{-1}$, U_0=0.75ms^{-1}, $f = 10^{-4}\text{s}^{-1}$.

lateral currents obtained from more realistic nonlinear hydrodynamic models with stratification (Lerczak and Geyer 2004; Burchard et al. 2011). A simple scaling for $\bar{V}$ can be developed by considering a range of nondimensional $\bar{V}$ based on solutions of the idealized model (Figure 4). For realistic $2 < h/\beta < 5$, normalized $\bar{V}$ is substantial with $\bar{V}\beta\sigma/(U_0 f/\sigma)^2/h_y$ often exceeding 0.005. Taking realistic parameters as above, this results in typical $\bar{V} \approx 5$ cm/s for $h_y = 0.01$. Below we furthermore show that variability of h/β from 2 to 8 across the estuary has an appreciable effect on the Lagrangian transport. Thus, our results suggest that lateral Lagrangian residual flows can play an important role in persistently transporting and organizing material over multiple tidal cycles in tidally driven estuaries, such as Delaware Bay, South San Francisco Bay, Mobile Bay, Raritan Bay, Hudson River, and James River.

c. Illustrative examples

We apply the idealized model to a parabolic channel with depth $h(y) = h_{\max} - (h_{\max} - h_{\min})(y/B)^2$, where B is half the channel width, and the maximum and minimum depths are, respectively, $h_{\max} = 15$ m and $h_{\min} = 5$ m (Figure 2). To explore the dependence on slope, we design three experiments with $B = 5$ km, 2 km, and 1 km with constant eddy viscosity of $A = 2.2 \times 10^{-3} \mathrm{m^2 s^{-1}}$. In these experiments, B controls the slope with steeper slopes for smaller B. To investigate model result for a greater h/β range, we also explore a case with smaller A of $A = 3.3 \times 10^{-4} \mathrm{m^2 s^{-1}}$, where B is set to $B = 2$ km. These A values are consistent with those from Lerczak and Geyer (2004), similar to other model parameters which are held constant at $U_0 = 0.75$ m s^{-1}, $f = 10^{-4}$ s^{-1}, and $T = 12$ h. For all cases, particles are released at $t = 0$ and $y = -B/2$ and tracked over six full semi-diurnal tidal cycles.

For the three experiments with greater A, h/β is in the range $h/\beta = 0.5 - 3$ so that the phase increases with depth (Figure 3). Consistent with the analysis above, particles converge in the channel center, even for the mildest sloping case with $B = 5$ km for which particles aggregate more slowly (Figure 5, upper six panels). As expected, the Stokes drift v_s is greater for steeper slopes (smaller B), so that the particles accumulate more quickly around channel center where $\partial\varphi/\partial y = 0$. In agreement with the analysis presented above, v_s accurately approximates $\bar{V}$ near the channel center but deviations between v_s and $\bar{V}$ are found away from the channel where slopes are steeper. These Lagrangian convergence zones quickly drive particles towards the channel center regardless of initial particle location (Figure 6a). As observed in Figure 1, particles surf the cross-channel velocity v_0 resulting in a net transport over a tidal cycle. Note that without tidal averaging particle aggregation zones oscillate around the channel center because of the tidal flow.

For the case with smaller A, h/β is in the range $h/\beta = 2 - 8$, which includes $h/\beta \approx 6$ at about $y \approx \pm 1000$ m. Since the phase is nearly constant at this cross-channel location with $\partial\varphi/\partial h = 0$ (Figure 3), the phase is also nearly constant across the channel and $\partial\varphi/\partial y = 0$. Consistently, Lagrangian convergence zones occur at those lateral locations where $h/\beta \approx 6$. As a consequence, particles converge for this case off the channel center at $y = \pm 1000$ m (Figure 5, bottom two panels), and particles that are evenly released over the channel aggregate in those two convergence zones (Figure 6b). In the channel center between $y \approx -1000$ m to $y \approx 1000$ m, the depth is deeper so that $h/\beta > 6$ here. In this region φ depends only weakly on h/β (Figure 3), so that particles converge

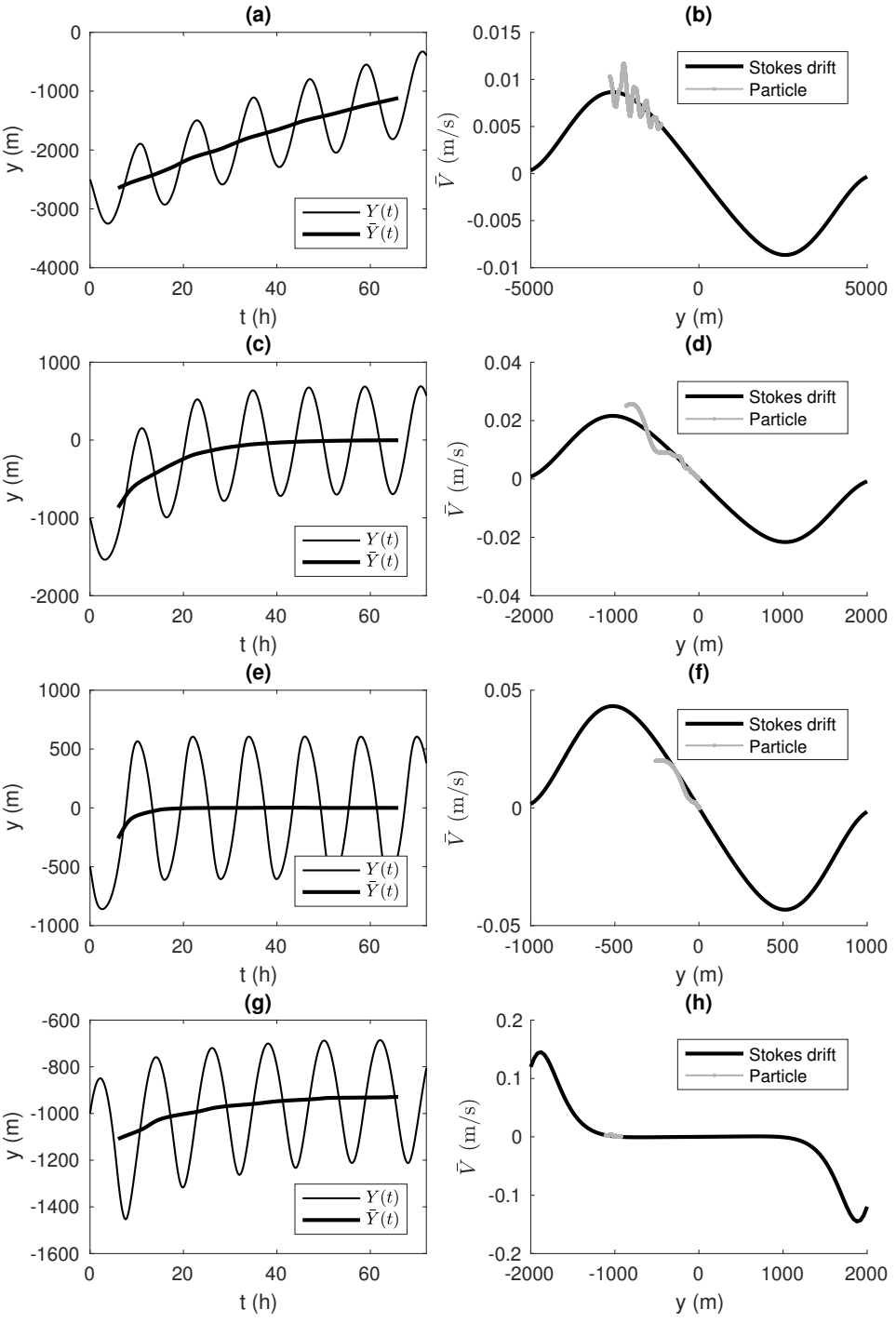

241 FIG. 5. Lagrangian cross-channel transport solutions with parabolic bathymetry with $h_{\max} = 15$ m, $h_{\min} = 5$
242 m and (a,b) $B = 5000$ m, $A = 2.2\times10^{-3}\mathrm{m^2s^{-1}}$; (c,d) $B = 2000$ m, $A = 2.2\times10^{-3}\mathrm{m^2s^{-1}}$; (e,f) $B = 1000$ m,
243 $A = 2.2\times10^{-3}\mathrm{m^2s^{-1}}$; (g,h) $B = 2000$ m, $A = 3.3\times10^{-4}\mathrm{m^2s^{-1}}$. (Left panels, a, c, e, g) Particle locations $Y(t)$ and
244 $\bar{Y}(t)$, (right panels b, d, f, h) $\bar{V}(y)$. Other model parameters are U_0=0.75ms^{-1}, $f = 10^{-4}\mathrm{s^{-1}}$, $T = 12$ h.

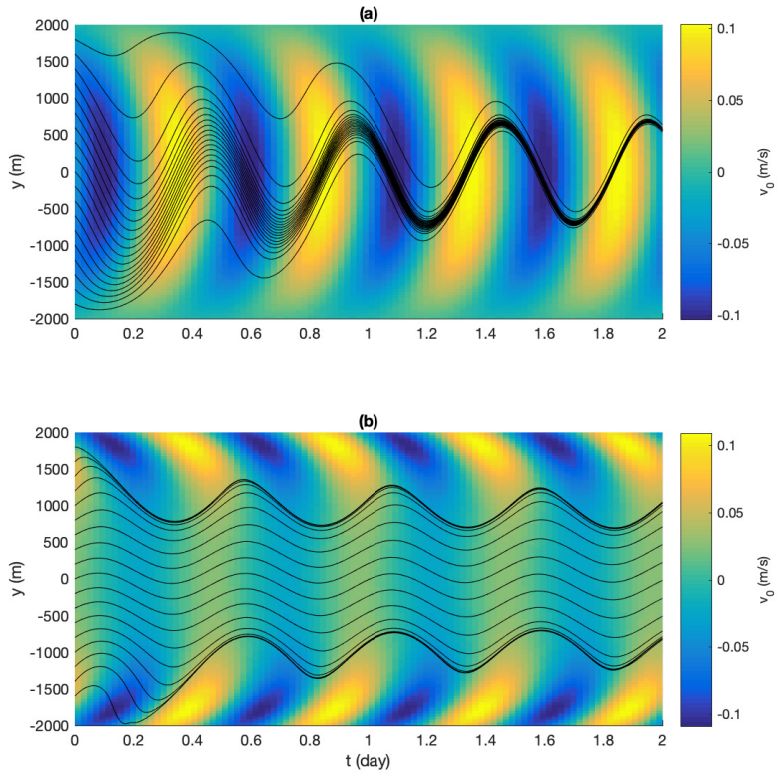

FIG. 6. Surface velocity v_0 and Particle trajectories $Y(t)$ (lines) for (a) $A = 2.2 \times 10^{-3} \mathrm{m^2 s^{-1}}$ with $\partial h/\partial y = 0$ and a convergence zone in the channel center at $y = 0$ m, and (b) $A = 3.3 \times 10^{-4} \mathrm{m^2 s^{-1}}$ and $\partial \varphi/\partial h = 0$ and convergence zones near $y \approx \pm 1000$ m; other parameters as discussed in the main text.

only slowly to the lateral location where $h/\beta \approx 6$ and particles are trapped between $y \approx -1000$ m to $y \approx 1000$ m for long times (Figure 6b). These results suggest that the Lagrangian residual transport and Lagrangian convergence zones strongly depend on turbulent boundary layer mixing (represented by A) and depth. The Stokes drift estimate is accurate for small $\bar{V}$ and thus insightful for identifying convergence regions.

Note that A may vary across the estuary due complex topography and related bottom roughness. For example, if roughness increases in shallower regions one may assume an inverse relation between A and h. If this inverse relation is approximated by $A \propto h^{-1}$ then $\beta \propto h^{-1/2}$ and $h/\beta \propto h^{3/2}$, which increases the phase change as the fluid moves across the channel relative to constant A (Figure 3) and thus enhances the Stokes drift.

5. Conclusions

This proof-of-concept study demonstrates the importance of Lagrangian residual velocities in transporting and aggregating surface trapped buoyant material in tidally driven estuaries. Any cross-estuary (lateral) Eulerian velocity with zero tidally averaged velocity yet with a lateral tidal phase variability will result in a net Lagrangian velocity that will follow this phase and converge at location where phase is most lagged, often the center of the channel. For small amplitude motions this velocity is characterized by Stokes velocity described by the low-order approximation in (2).

A straightforward analysis of the lateral momentum balance reveals that the tidal phase generally depends on tidal frequency, turbulent mixing, and estuary depth. For greater depth and tidal frequency but weaker turbulent mixing, the lateral acceleration increases relative to the stress divergence term, inducing a phase shift of the later velocity towards 90° out of phase with the Coriolis force term. Therefore, the tidal phase varies across the estuary with varying estuarine depth. Our results show that this lateral phase variability has critical implications for the lateral transport and aggregation of surface trapped material. For steeper bathymetry, the lateral change in tidal phase is greater and the corresponding lateral Lagrangian residual flow faster. At local depth extrema, e.g. in the thalweg, depth does not vary laterally, so that the associated tidal phase is laterally constant. Therefore, the Stokes drift is weak near depth extrema resulting in Lagrangian convergence zones where buoyant material concentrates.

We examined these ideas employing the idealized analytic model from Lerczak and Geyer (2004) in which the along-estuary tidal flow is driven by an imposed barotropic pressure gradient, whereas cross-estuary flow is induced by the Coriolis force. Analytic solutions of the lateral tidal phase and nondimensional velocity at the surface only depend on a nondimensional depth given by the estuarine depth normalized by a tidally driven turbulent boundary layer depth scale. The nondimensional Stokes drift also only depends on this nondimensional depth and the Stokes drift is proportional to the bathymetry slope. Therefore, the Stokes drift changes sign across depth maxima coinciding with a Lagrangian convergence zone. Furthermore, analytic phase solutions demonstrate a local peak of lateral phase at a particular normalized depth revealing Stokes drift convergence across the channel that is not related to bathymetry extrema but may occur away from the channel center. Although the Stokes drift is only an accurate estimate for the Lagrangian residual

velocity for smaller amplitude motions, and thus smaller slopes, it still provides expectations for Lagrangian convergence zones.

More comprehensive approaches need to incorporate competing influences due to density variations and lateral advection, which affects the lateral circulation and mixing in the estuary. Some mixing modifications due to stratifications may be captured by adjusting A, and thus β, though others may require that A depends on the tidal phase and vertical coordinate (Jay and Musiak 1994). Furthermore, differential advection of saltier or fresher water induce lateral density gradients and associated Eulerian secondary circulations (Nunes and Simpson 1985; MacCready and Geyer 2010) that could either reinforce or compete with Lagrangian convergence zones. Note that even in the presence of variable densities, the tidal phase of the lateral circulation still generally depends on cross-channel location which will introduce Lagrangian residual flows focus of our study.

Overall, this study highlights that convergence zones due to Lagrangian residual velocities are efficient in forming persistent aggregation regions of buoyant material along the estuary and should be taken into account for comprehensive estuarine transport investigations.

Acknowledgments. This work was supported by the U.S. National Science Foundation (grant OCE-2148370). We would like to thank two anonymous reviewers for important and constructive comments that have improved this manuscript.

Data availability statement. This research is based on theoretical work without numerical or observational data sets that can be shared beyond what is presented here.

References

Buhler, O., 2009: *Waves and Mean Flows*. Cambridge University Press, https://doi.org/10.1017/cbo9781107478701, URL https://doi.org/10.1017%2Fcbo9781107478701.

Burchard, H., R. D. Hetland, E. Schulz, and H. M. Schuttelaars, 2011: Drivers of residual estuarine circulation in tidally energetic estuaries: Straight and irrotational channels with parabolic cross section. *Journal of Physical Oceanography*, **41 (3)**, 548–570, https://doi.org/10.1175/2010jpo4453.1, URL https://doi.org/10.1175%2F2010jpo4453.1.

Cohen, J. H., A. M. Internicola, R. A. Mason, and T. Kukulka, 2019: Observations and simulations of microplastic debris in a tide, wind, and freshwater-driven estuarine environment: the delaware bay. *Environmental Science & Technology*, **53 (24)**, 14 204–14 211, https://doi.org/10.1021/acs.est.9b04814, URL https://doi.org/10.1021%2Facs.est.9b04814.

Feng, S., R. T. Cheng, and X. Pangen, 1986: On tide-induced lagrangian residual current and residual transport: 1. lagrangian residual current. *Water Resources Research*, **22 (12)**, 1623–1634.

Garrett, C., 2004: Tidal rectification and stokes drift. *Woods Hole Oceanographic Institution Geophysical Fluid Dynamics*, https://gfd.whoi.edu/gfd-publications/gfd-proceedings-volumes/2004-2/, Vol. Proceedings Volume 2004, Lecture 8.

Jay, D. A., 1991: Estuarine salt conservation: A lagrangian approach. *Estuarine, Coastal and Shelf Science*, **32 (6)**, 547–565.

Jay, D. A., and J. D. Musiak, 1994: Particle trapping in estuarine tidal flows. *Journal of Geophysical Research: Oceans*, **99 (C10)**, 20 445–20 461, https://doi.org/https://doi.org/10.1029/94JC00971, URL https://agupubs.onlinelibrary.wiley.com/doi/abs/10.1029/94JC00971, https://agupubs.onlinelibrary.wiley.com/doi/pdf/10.1029/94JC00971.

Kennish, M. J., 2002: Environmental threats and environmental future of estuaries. *Environmental Conservation*, **29 (1)**, 78–107, https://doi.org/10.1017/S0376892902000061.

LeBlond, P. H., 1978: On tidal propagation in shallow rivers. *Journal of Geophysical Research: Oceans*, **83 (C9)**, 4717–4721.

Lemagie, E. P., and J. A. Lerczak, 2015: A comparison of bulk estuarine turnover timescales to particle tracking timescales using a model of the yaquina bay estuary. *Estuaries and Coasts*, **38 (5)**, 1797–1814.

Lerczak, J. A., and W. R. Geyer, 2004: Modeling the lateral circulation in straight, stratified estuaries. *Journal of Physical Oceanography*, **34 (6)**, 1410–1428, https://doi.org/10.1175/1520-0485(2004)034<1410:mtlcis>2.0.co;2, URL https://doi.org/10.1175%2F1520-0485%282004%29034%3C1410%3Amtlcis%3E2.0.co%3B2.

Li, C., and J. O'Donnell, 1997: Tidally driven residual circulation in shallow estuaries with lateral depth variation. *Journal of Geophysical Research: Oceans*, **102 (C13)**, 27 915–27 929.

Li, M., P. Cheng, R. Chant, A. Valle-Levinson, and K. Arnott, 2014: Analysis of vortex dynamics of lateral circulation in a straight tidal estuary. *Journal of Physical Oceanography*, **44 (10)**, 2779–2795, https://doi.org/10.1175/jpo-d-13-0212.1, URL https://doi.org/10.1175%2Fjpo-d-13-0212.1.

Longuet-Higgins, M., 1969: On the transport of mass by time-varying ocean currents. *Deep Sea Research and Oceanographic Abstracts*, **16 (5)**, 431–447, https://doi.org/https://doi.org/10.1016/0011-7471(69)90031-X, URL https://www.sciencedirect.com/science/article/pii/001174716990031X.

MacCready, P., and W. R. Geyer, 2010: Advances in estuarine physics. *Annual Review of Marine Science*, **2 (1)**, 35–58, https://doi.org/10.1146/annurev-marine-120308-081015, URL https://doi.org/10.1146%2Fannurev-marine-120308-081015.

Nunes, R., and J. Simpson, 1985: Axial convergence in a well-mixed estuary. *Estuarine, Coastal and Shelf Science*, **20 (5)**, 637–649, https://doi.org/https://doi.org/10.1016/0272-7714(85)90112-X, URL https://www.sciencedirect.com/science/article/pii/027277148590112X.

Ridderinkhof, H., and J. Zimmerman, 1992: Chaotic stirring in a tidal system. *Science*, **258 (5085)**, 1107–1111.

Valle-Levinson, A., 2008: Density-driven exchange flow in terms of the kelvin and ekman numbers. *Journal of Geophysical Research: Oceans*, **113 (C4)**.

Zimmerman, J., 1979: On the euler-lagrange transformation and the stokes' drift in the presence of oscillatory and residual currents. *Deep Sea Research Part A. Oceanographic Research Papers*, **26 (5)**, 505–520, https://doi.org/https://doi.org/10.1016/0198-0149(79)90093-1, URL https://www.sciencedirect.com/science/article/pii/0198014979900931.